Lunar Rover Power Electronic System

Hubers, Martijn ; Gagic, Mladen; Shekhar, Aditya

DOI
10.1109/IECON51785.2023.10312700

Publication date
2023

Document Version
Final published version

Published in
Proceedings of the IECON 2023- 49th Annual Conference of the IEEE Industrial Electronics Society

Lunar Rover Power Electronic System

Martijn Hubers, Mladen Gagic and Aditya Shekhar
Dept. Electrical Sustainable Energy - Delft University of Technology, The Netherlands

IECON 2023- 49th Annual Conference of the IEEE Industrial Electronics Society | 979-8-3503-3182-0/23/$31.00 ©2023 IEEE | DOI: 10.1109/IECON51785.2023.10312700

***Abstract*—The small, light-weight and modular Lunar rover must survive several earth days in harsh environment after its moon landing. Its power electronic system with integrated solar generation needs power for its mission and also to stay warm in very cold temperatures of the moon. This paper presents the design of the power electronic system of the Lunar Zebro rover. Two topologies are compared that result from using a 12 V bus and 24 V bus. The design of the DC/DC converters required is presented for CCM and DCM operation. The losses in the DC/DC converters operating in CCM and DCM are calculated for the two bus voltages to determine the mode of operation and bus voltage that results in the highest efficiency. Further, the average power loss during operation of the rover is estimated for both bus voltages. Operating the DC/DC converters in CCM using a 12 V bus results in the lowest losses.**

***Index Terms*—DC-DC Converters; Buck; Boost; Buck-Boost; Bidirectional; DCM; CCM; Efficiency; Power Electronic System ; Moon Rover.**

I. Introduction

Exploration of the moon has regained interest recently [1]. The Artemis program of NASA has as its goal to send humans to the moon yearly to establish surface capabilities [2], while SpaceX is also planning to land humans on the moon with Starship [3]. The radiation-rich environment on the moon poses serious health risks for astronauts [4]. Locations with the least amount of radiation will be most suitable to establish moon bases. To find these locations, a map of the radiation environment on the moon is required. This is the goal of the Lunar Zebro project, which will ultimately send a swarm of small, lightweight rovers to map the radiation environment on the moon [5].

The power electronic system is one of the most critical systems of the Lunar Zebro rover. It must be able to store energy, is responsible for supplying power to all subsystems inside the rover, and should charge the batteries from the PV panels mounted on top of the rover. In addition, it must operate in the harsh conditions of the moon. The radiation environment on the moon can cause early failure in power electronic components [6]. Furthermore, it must be able to withstand the extreme temperatures on the moon, ranging from -250°C at the poles during the night to +120°C at the equator during the day [7].

In a system where multiple sources and loads are interconnected, it is common practice to have a central DC bus [8]–[10]. This has several advantages. First of all, the power flowing into and out of the batteries is controlled using a single DC/DC converter. Secondly, the system is made modular as additional systems can be connected to the DC bus. Finally, the input voltage of the DC/DC converters for the 12 V, 5 V, and 3.3 V output are regulated instead of the fluctuating battery voltage. This simplifies the design of these converters.

The value of the DC bus voltage will influence the design and efficiency of the power electronic system, as well as the topology, the type of DC/DC converters required, the voltage rating of the components, the efficiency of each DC/DC converter, and the system efficiency during operation. The efficiency is a key parameter, as a higher efficiency results in longer operation of the rover. Furthermore, the temperature rise in the components is reduced, increasing their reliability and reducing the size of the heat-sink [11].

The DC/DC converters are operated in Continuous Conduction Mode (CCM) or Discontinuous Conduction Mode (DCM). In CCM, the current ripple in the inductor is smaller, reducing the core losses, and reducing the conduction losses in the switch, diode, and output capacitor. However, the inductor required is larger, increasing the winding resistance thus the conduction losses [11] [12]. In DCM, the switch turns on at zero current and without diode reverse recovery current, which reduces the switching losses [13]. However, the inductor current ripple is increased, increasing the conduction losses in the switch, diode, and output capacitor, as well as the core losses in the inductor [14] [15].

In this paper, the power electronic system that results in the highest efficiency is determined. This is done by modelling the losses in the two topologies operating in CCM and DCM. The losses in the DC/DC converters are modelled, as well as the average power loss during operation. The paper is structured as follows. First, in Section II, an overview of the power electronic system is given, discussing the topology using a 12 V and 24 V DC bus. Next, in Section III, the design of the DC/DC converters is discussed. In Section IV, the losses in each DC/DC converter are modelled. Section V discusses the system efficiency for the two bus voltages based on the usage profile of the rover. Finally, Section VI gives conclusions.

II. Overview Power Electronic System

The power electronic system can be divided into the following subsystems:

- The battery pack, consisting of five Panasonic NCR18650B batteries in series.
- The PV panel, capable of generating 18.12 W of power
- The bidirectional converter connected to the battery
- The DC/DC converter connected to the PV panel
- The buck converter that regulates the 12 V output

The authors are with the department of Electrical Sustainable Energy in the DCE&S Group at Delft University of Technology. For contact email: a.shekhar@tudelft.nl.

- The buck converter that regulates the 5 V output
- The buck converter that regulates the 3.3 V output

A bus voltage of 12 V and 24 V is considered. Because the voltage of the battery pack varies between 13.5 V and 21 V, a bus voltage in between this range results in a bidirectional buck-boost converter. This is undesirable, because a buck-boost converter results in larger voltage stress, thus more losses than a buck or boost converter [16].

A. 12 V bus

The topology using a 12 V bus is shown in Figure 1. The bidirectional converter always operates in buck mode when discharging the batteries. No DC/DC converter is required for the 12 V output. However, a buck-boost converter is required for the PV panel.

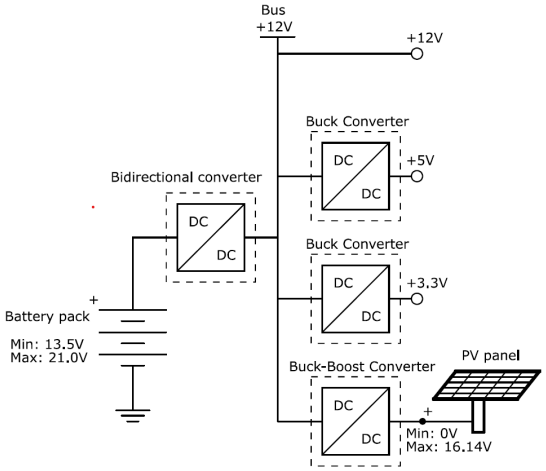

Fig. 1: Topology using a 12 V bus

B. 24 V bus

The topology using a 24 V bus is shown in Figure 2. Discharging the batteries results in boost operation of the bidirectional converter. At the PV panel, a boost converter is required. This results in fewer losses than the buck-boost converter of the 12 V bus. Furthermore, the conduction losses in the DC bus are reduced. However, a buck converter is required for the 12 V output, which introduces additional losses.

III. Design DC/DC Converters

The design of the DC/DC converters required for a 12 V bus and 24 V bus is discussed next. The design equations from [17] are used to calculate the inductance and capacitance required for CCM and DCM. A switching frequency of 100 kHz is used.

A. Buck Converter

The buck converters in CCM are designed to operate at BCM at I_{BCM}=12.5%$I_{\text{o,max}}$=0.5 A. For DCM, the inductance is calculated at maximum output current to always operate in DCM. The output voltage ripple is maximum at maximum

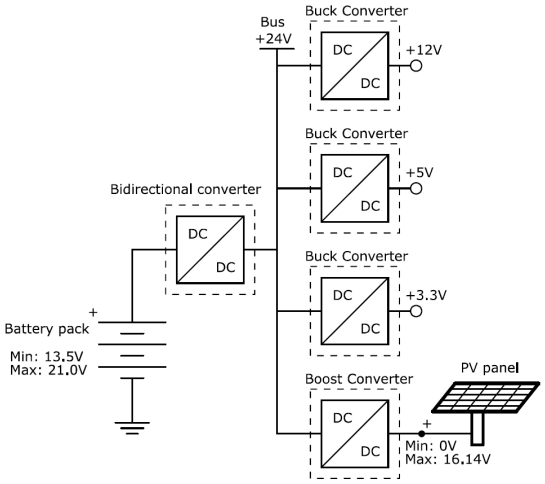

Fig. 2: Topology using a 24 V bus

load current, hence the capacitance is calculated at maximum output current as well

B. Boost Converter

For the boost converter operating in CCM, the inductance and capacitance required is largest when V_{in} = 0.5V_{o}. To limit the size of the inductor in CCM, the inductor current ripple is set at $I_{\text{BCM}} = 25\% I_{\text{in,max}}$ to operate in BCM. Similar as for the buck converter in DCM, the inductance and capacitance in DCM are calculated at maximum load current. The inductance reduces for smaller PV panel voltages until it becomes 0 μH. This implies that a limit must be set for the PV panel voltage for the converter to start operating in DCM. This limit is set at 20% of $P_{\text{pv,max}}$, so at $V_{\text{pv}} \approx 3\,V$. The capacitance is calculated at Maximum Power Point (MPP), where $V_{\text{pv}} = 15.14\,V$ and $I_{\text{pv}} = 1.197\,A$.

C. Buck-Boost Converter

For the buck-boost converter in CCM, the inductance required is largest when V_{in} = V_{o}. The converter operates in BCM at $I_{\text{BCM}} = 20\% I_{\text{o,max}}$. The output capacitance required is largest at MPP. For DCM, the same operating conditions are applicable as for the boost converter in DCM to obtain the worst-case conditions.

D. Bidirectional Converter

For the 12 V bus, the bidirectional converter operates in buck mode when discharging the batteries. Because the power is larger when discharging than when charging, the design is based on discharging mode. Hence, the design steps are the same as for the buck converter. The worst-case condition occurs at maximum battery voltage. For the 24 V bus, the bidirectional converter operates in boost mode when discharging the batteries. In this case, the worst-case condition occurs at minimum battery voltage. Because this converter has the largest power rating, $I_{\text{o,min}}$=10%$I_{\text{o,max}}$ to limit the current ripple and thus the conduction losses.

E. Specifications and Component Values

The specifications of each converter for a 12 V and 24 V bus is shown in Table I. The resulting values of inductance and capacitance calculated and used are shown in Table II.

TABLE I: Specifications of the DC/DC converters

	P_o [W]	V_{in} [V]	V_o [V]	$I_{o,max}$ [A]	I_{BCM} [A]	ΔV_o [V]
Bus	*Bidirectional*					
12V	90.22	13.5 to 21	12	7.519	0.752	0.12
24V	90.22	13.5 to 21	24	3.759	0.376	0.24
	PV converter					
12V	18.12	0 to 16.14	12	1.51	0.302	0.12
24V	18.12	0 to 16.14	24	0.755	0.151	0.24
	3.3V buck					
12V	13.20	12	3.3	4	0.5	0.033
24V	13.20	24	3.3	4	0.5	0.033
	5V buck					
12V	20	12	5	4	0.5	0.05
24V	20	24	5	4	0.5	0.05
	12V buck					
24V	48	24	12	4	0.5	0.12

TABLE II: Calculated and used inductor and capacitor values, for each converter for a 12 V and 24 V bus in CCM and DCM

		L calc [μH]	L used [μH]	C calc [μF]	C used [μF]
Bus		*Bidirectional*			
12V	**CCM**	34.2	47	11.4	15
	DCM	0.887	0.47	415.81	594
24V	**CCM**	44.19	47	68.53	99
	DCM	3.06	2.2	100.64	132
		PV converter			
12V	**CCM**	62.66	75	55.65	68
	DCM	8.02	6.8	66.39	100
24V	**CCM**	125.31	150	15.73	22
	DCM	10.97	10	19.81	22
		3.3V buck			
12V	**CCM**	23.93	33	27.46	33
	DCM	2.99	2.2	395.42	400
24V	**CCM**	28.46	33	32.67	47
	DCM	3.56	3.3	325.81	400
		5V buck			
12V	**CCM**	29.17	33	22.10	33
	DCM	3.65	3.3	219.9	220
24V	**CCM**	39.58	47	21.05	33
	DCM	4.95	4.7	210.28	220
		12V buck			
24V	**CCM**	60	75	8.33	15
	DCM	7.5	6.8	91.49	100

The choice of inductors is based on the SGIHLP series from Vishay. The capacitors are selected from the Kyocera AVX high reliability tantalum capacitors series. These inductors and capacitors are available in space-grade and non-space-grade variants. For the bidirectional converter, the EPC2014C GaN switches are used. For the other converters, the EPC8004 GaN switches are used. Various Si Schottky diodes are used for the converters.

IV. Losses in DC/DC converters

The losses in the switch, diode, inductor, and output capacitor are considered to determine which bus voltage and mode of operation results in the highest efficiency of each converter.

A. Losses in the switch

The losses in the switch consist of conduction losses and switching losses. The conduction losses are calculated in (1).

$$P_{\text{sw,cl}} = I_{\text{sw,rms}}^2 R_{\text{DS}} \tag{1}$$

Here, $I_{\text{sw,rms}}$ is the RMS current in the switch, and R_{DS} the drain-source on-resistance. The switching losses are calculated in (2).

$$P_{\text{sw,fs}} = (E_{\text{on}} + E_{\text{off}}) F_{\text{s}} \tag{2}$$

Here, F_{s} is the switching frequency, and E_{on} and E_{off} the turn-on and turn-off switching energy loss, respectively. These are calculated using (3) and (4).

$$E_{\text{on}} = \frac{1}{2} V_{\text{sw,off}} I_{\text{sw,on}} t_{\text{on}} \tag{3}$$

$$E_{\text{off}} = \frac{1}{2} V_{\text{sw,off}} I_{\text{sw,off}} t_{\text{off}} \tag{4}$$

Here, $V_{\text{sw,off}}$ is the voltage the switch blocks when turned off, $I_{\text{sw,on}}$ and $I_{\text{sw,off}}$ the current that the switch must switch when turned on and off, respectively. Because $I_{\text{sw,on}} = 0$ in DCM, only turn-off losses occur in DCM. Finally, t_{on} and t_{off} are the turn-on and turn-off times of the switch.

B. Losses in the diode

The losses in the diode consist of conduction losses and switching losses as well. The conduction losses are due to the forward voltage drop and on-resistance of the diode and is calculated using (5).

$$P_{\text{D,cl}} = V_{\text{f}} I_{\text{D,av}} + I_{\text{D,rms}}^2 R_{\text{D,on}} \tag{5}$$

Here, V_{f} is the forward voltage drop of the diode, $I_{\text{D,av}}$ the average diode current, $I_{\text{D,rms}}$ the RMS diode current, and $R_{\text{D,on}}$ the on-resistance of the diode. The switching losses are due to the junction capacitance and due to reverse recovery current. However, since Schottky diodes are used, the reverse recovery current can be neglected. Thus, the switching losses in the diode are calculated using (6).

$$P_{\text{D,fs}} = \frac{1}{2} C_{\text{j}} V_{\text{R}}^2 F_{\text{s}} \tag{6}$$

Here, C_{j} is the junction capacitance, V_{R} the reverse voltage blocked, and F_{s} the switching frequency.

C. Losses in the inductor

The losses in the inductor considered are the DC conduction losses and core losses, neglecting the AC winding losses. The DC conduction losses are calculated using (7).

$$P_{\text{L,DC}} = I_{\text{L,rms}}^2 R_{\text{DC}} \tag{7}$$

Here, $I_{\text{L,rms}}$ is the RMS inductor current, and R_{DC} the DC resistance of the inductor. The core losses in CCM are evaluated using the core loss calculator provided by Vishay

[18]. This tool calculates the core losses for CCM only. For DCM, the core losses are calculated using the generalised Steinmetz equation, shown in (8).

$$P_{\mathrm{v}} = V_{\mathrm{e}} \frac{k_{\mathrm{i}} \left(\Delta B\right)^{\beta-\alpha}}{T_{\mathrm{s}}} \cdot \left(\left| \frac{\Delta B}{D T_{\mathrm{s}}} \right|^{\alpha} D T_{\mathrm{s}} + \left| \frac{\Delta B}{(1-D)\, T_{\mathrm{s}}} \right|^{\alpha} (1-\mathrm{D})\, T_{\mathrm{s}} \right) \tag{8}$$

The Steinmetz coefficients α, β, and k are obtained from curve fitting the core losses in CCM using the core loss tool from Vishay. Further, V_{e} is the effective core volume, and ΔB the change in flux density, shown in (9).

$$\Delta B = L \frac{\Delta I_{\mathrm{L}}}{N A_{\mathrm{c}}} \tag{9}$$

Here, N is the number of turns of the inductor, A_c is the area of the cross-section of the bobbin of the magnetic core, and ΔI_{L} is the current ripple in the inductor.

D. Losses in the output capacitor

The losses in the output capacitor considered are conduction losses only. They are calculated in (10).

$$P_{\mathrm{Co}} = I_{\mathrm{Co,rms}}^2 R_{\mathrm{ESR}} \tag{10}$$

Here, $I_{\mathrm{Co,rms}}$ is the RMS current in the capacitor, and R_{ESR} the equivalent series resistance of the output capacitor.

E. Results

The losses in each component for the converters operating in CCM and DCM for the 12 V and 24 V bus are shown as a stacked bar graph in Figure 3. The losses are shown as a percentage of the power rating of the corresponding converter. For all converters holds that operating in CCM results in higher efficiency than operating in DCM. This is mainly due to the significant decrease of the losses in the inductor. The losses in the inductor are significantly larger for DCM, which is caused by the significant increase of the core losses. In [14] it is shown that the core losses in DCM can reduce the efficiency up to 10%. All the calculated currents where verified using simulations in Matlab Simulink.

For the bidirectional converter, only for DCM operation the 24 V bus results in a notably increased efficiency. From Figure 3, the losses in the switch and output capacitor in DCM are reduced significantly for the 24 V bus. This is caused by the reduction of the currents due to the increased bus voltage.

Similarly, the PV converter is more efficient for a 24 V bus. This is expected because the PV converter is a boost converter for the 24 V bus, which is in general more efficient than the buck-boost converter used for the 12 V bus [19] [20]. Again, the increase in efficiency is most prominent for DCM. In DCM, the losses in each component are reduced significantly. In CCM, the losses in the switch and diode are reduced. However, the inductor losses are increased because the inductance used is doubled, resulting in significantly more conduction losses.

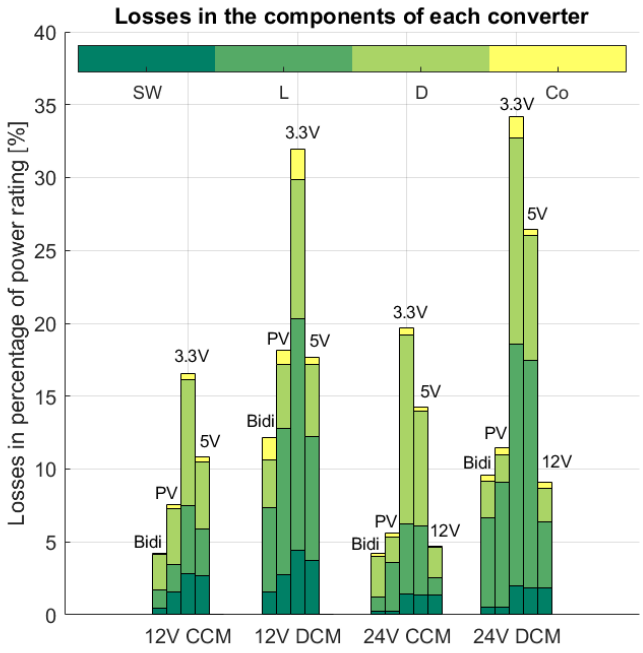

Fig. 3: Losses in the switch (SW), inductor (L), diode (D), and output capacitor (Co) of the bidirectional (Bidi), PV buck or buck-boost converter (PV), 3.3 V buck (3.3V), 5 V buck (5V), and 12 V buck (12V) converters. The losses are presented as a percentage of the rated power of the corresponding converter.

On the other hand, for the 5 V and 3.3 V buck converters, operating at a 12 V bus results in higher efficiency. This is mainly due to the reduced losses in the diode. The duty cycle is higher for the 12 V bus, so the diode conducts for a shorter amount of time while the switch conducts longer. The conduction losses in the diode are usually larger than the conduction losses in the switch due to the contribution of the forward voltage drop in the diode [11]. To improve the efficiency, synchronous rectification can be implemented [21]. As expected, the the losses in the switch of the 12 V bus are increased compared to the 24 V bus because the duty cycle is larger for the 12 V bus.

The 3.3 V buck converter has remarkably low efficiencies, mainly in DCM. This can be accounted for the fact that the power rating is low (13.2 W) while the current is relatively large (4 A). Therefore, the conduction losses make up a significant part of the total power. Furthermore, the core losses of the inductor in DCM are 1.81 W and 1.85 W for the 12 V and 24 V bus, respectively. This corresponds to a 13.7% and 14.0% drop in the efficiency. From Figure 4 can be seen that the losses in the 3.3 V, 5 V, and 12 V buck converters differ by less than 1 W. This small difference is because different components are used. Therefore, the low efficiency of the 3.3 V buck converter is acceptable.

In [22], a synchronous buck converter operating in CCM at 1.2 V and 6 A output has a measured efficiency of 95%. It

is found that approximately 80% of the losses in the diodes of the 5 V and 3.3 V buck converters are due to the forward voltage drop. Thus, it is expected that these converters in CCM approach a 90% efficiency when operated in synchronous topology, which is in good agreement with [22].

The losses in each converter for both bus voltages and mode of operations are summed up to determine which bus voltage results in the lowest total losses. This is shown in Figure 4. Operating in CCM with a 12 V bus results in fewer losses than the 24 V bus in CCM. Similarly, operating in DCM with a 12 V bus results in fewer losses than a 24 V bus. For CCM, even without the 12 V buck converter considered for the 24 V bus, the 24 V bus results in more total losses. For DCM, adding the 12 V buck converter with the 24 V bus results in more losses using the 24 V bus. For both the 12 V and 24 V bus, operating in CCM is more efficient than operating in DCM and results in the lowest total losses. Therefore, the converters will be operated in CCM. Furthermore, the 12 V bus results in 3 W fewer losses than the 24 V bus in CCM.

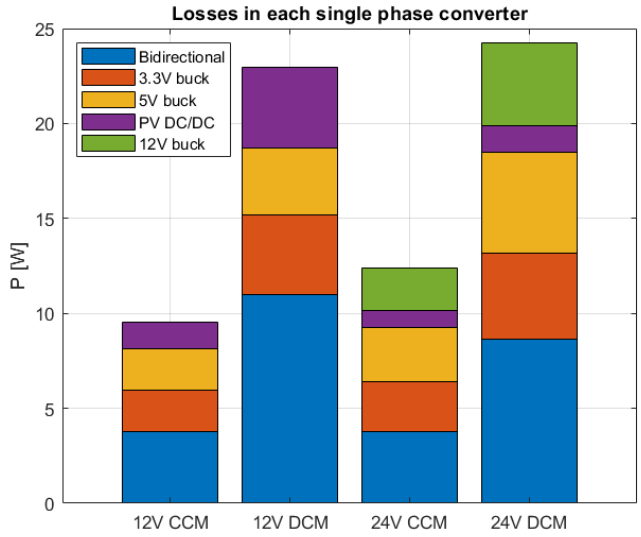

Fig. 4: Losses in the converters for a 12 V bus and 24 V bus operating in CCM and DCM

V. Losses Based on Usage Profile

To verify if the 12 V bus results in fewer losses than the 24 V bus, the overall efficiency of the 12 V and 24 V DC bus is compared based on the usage profile of the rover. This is done by calculating the average power loss during one operational cycle. One operational cycle means that the fully charged batteries are first fully discharged at constant load without energy generated from the PV panel, after which they are completely charged from the PV panel at maximum power point without any loads. This is a realistic usage scenario because the rover does not operate while charging. The influence of adding the 12 V buck converter but having a more efficient boost converter for the 24 V DC bus topology will be compared to the 12 V DC bus topology, where a less efficient buck-boost converter is used but no 12 V buck converter is required. This is done for the DC/DC converters operating in CCM because it was found to be more efficient than operating in DCM. The following assumptions are made:

- The efficiency of the 5 V and 3.3 V buck converter remains unaffected by the change in bus voltage, and their contribution to the average power loss is equal for a 12 V bus and 24 V bus.
- The efficiency of the bidirectional is the same during charging and discharging.
- 80% of the battery pack capacity E_{bp} is used for walking, which has a capacity of E_{bp}=57.60 Wh.
- The average output power drawn by the 12 V output is 12 W

The average power loss during one operational cycle is calculated using (11).

$$P_{\text{L,av}} = \frac{E_{\text{L,w}} + E_{\text{L,ch}}}{t_{\text{cycle}}} = \frac{P_{\text{L,w}} t_{\text{w}} + P_{\text{L,ch}} t_{\text{ch}}}{t_{\text{w}} + t_{\text{ch}}} \tag{11}$$

Here, $E_{\text{L,w}}$ is the total energy loss in the 12 V buck converter during walking, and $E_{\text{L,ch}}$ is the total energy loss in the DC/DC converter of the PV panel during charging. Similarly, $P_{\text{L,w}}$ and $P_{\text{L,ch}}$ are the power losses during walking and charging in the corresponding DC/DC converters, and t_{w} and t_{ch} are the times the rover walks and charges, respectively. Using (12) and (13), $P_{\text{L,w}}$ and $P_{\text{L,ch}}$ are calculated.

$$P_{\text{L,w}} = P_{\text{L,12V,w}} + P_{\text{L,bi,w}} \tag{12}$$

$$P_{\text{L,ch}} = P_{\text{L,pv,ch}} + P_{\text{L,bi,ch}} \tag{13}$$

Here, $P_{\text{L,12V,w}}$ and $P_{\text{L,bi,w}}$ are the losses in the 12 V buck converter and bidirectional converter during discharging. Similarly, $P_{\text{L,pv,ch}}$ and $P_{\text{L,bi,ch}}$ are the losses in the PV DC/DC converter and bidirectional converter during charging. These are calculated using (14)-(17).

$$P_{\text{L,12V,w}} = P_{\text{12V}} \left(\frac{1}{\eta_{\text{12V}}} - 1 \right) \tag{14}$$

$$P_{\text{L,bi,w}} = \frac{P_{\text{12V}}}{\eta_{\text{12V}}} \left(\frac{1}{\eta_{\text{bi}}} - 1 \right) \tag{15}$$

$$P_{\text{L,pv,ch}} = P_{\text{PV}} \left(1 - \eta_{\text{pv}}\right) \tag{16}$$

$$P_{\text{L,bi,ch}} = P_{\text{PV}} \eta_{\text{pv}} \left(1 - \eta_{\text{bi}}\right) \tag{17}$$

Here, η_{12V}, η_{bi}, and η_{pv} are the efficiencies of the 12 V buck, bidirectional, and the PV DC/DC converter, respectively. Further, P_{PV}=18.12 W is the maximum power generated from the PV panel, and P_{12V}= 12W the average power drawn by the 12 V output. The time in seconds the rover can walk and needs to charge is calculated using (18) and (19).

$$t_{\text{w}} = \frac{0.8 E_{\text{bp}} \eta_{\text{bi}} \eta_{\text{12V}}}{P_{\text{12V}}} \cdot 3600 \tag{18}$$

$$t_{\text{ch}} = \frac{E_{\text{bp}}}{P_{\text{PV}}\eta_{\text{pv}}\eta_{\text{bi}}} \cdot 3600 \tag{19}$$

The nominator of (18) represents the energy that is available from the battery pack at the output of the 12 V buck converter. The efficiencies obtained in Section IV for CCM of the 12 V buck converter, bidirectional, and PV DC/DC converter are used in (14)-(19).

The 12 V bus results in an average power loss of 1.47 W, while the 24 V bus results in an average power loss of 1.50 W. Thus, the 12 V bus results in 30 mW less average losses. Since both the losses in the DC/DC converters and the average power loss are lower for the 12 V bus, it can be concluded that the 12 V bus is the best choice for the bus voltage. Therefore, operating the DC/DC converters in CCM with a bus voltage of 12 V results in a power electronics system with the highest efficiency.

VI. Conclusion

In this paper, the design of the EPS of the Lunar Zebro is presented. The design of the DC/DC converters in the EPS for CCM and DCM are presented, both for a bus voltage of 12 V and 24 V. Further, the losses in the EPS are calculated. First, the losses in each DC/DC converter in the EPS are calculated. For both the 12 V bus and 24 V bus, CCM results in fewer losses than DCM. Hence, the DC/DC converters will be operated in CCM. Furthermore, the 12 V bus results in fewer total losses in the DC/DC converters than the 24 V bus. Secondly, the average losses during operation are calculated. It is found that a 12 V bus results in 30 mW fewer losses on average than a 24 V bus. Therefore, because both the losses in the DC/DC converters and average power losses during operation are lower for a 12 V bus, this bus voltage will be used for the Lunar Zebro rover.

References

[1] NASA, "Nasa's first flight with crew important step on long-term return to the moon, missions to mars," https://www.nasa.gov/feature/nasa-s-first-flight-with-crew-important-step-on-long-term-return-to-the-moon-missions-to, accessed: 2023-04-28.

[2] M. Smith, D. Craig, N. Herrmann, E. Mahoney, J. Krezel, N. McIntyre, and K. Goodliff, "The artemis program: An overview of nasa's activities to return humans to the moon," in *2020 IEEE Aerospace Conference*, 2020, pp. 1–10.

[3] "The moon, returning humans to lunar missions," https://www.spacex.com/human-spaceflight/moon/, accessed: 2023-04-28.

[4] M. Durante and F. A. Cucinotta, "Physical basis of radiation protection in space travel," *Rev. Mod. Phys.*, vol. 83, pp. 1245–1281, Nov 2011. [Online]. Available: https://link.aps.org/doi/10.1103/RevModPhys.83.1245

[5] "Lunar zebro world's smallest and lightest rover yet, built by tu delft students," zebro.space, accessed: 2023-04-28.

[6] U. Scheuermann and U. Schilling, "Impact of device technology on cosmic ray failures in power modules," *IET Power Electronics*, 2016.

[7] NASA, "North pole - nasa's lunar reconnaissance orbiter," https://lunar.gsfc.nasa.gov/images/lithos/LROlitho7temperaturevariation27May2014.pdf, 2014.

[8] M. D'Antonio, C. Shi, B. Wu, and A. Khaligh, "Design and optimization of a solar power conversion system for space applications," *IEEE Transactions on Industry Applications*, vol. 55, no. 3, pp. 2310–2319, 2019.

[9] V. A. Prabhala, B. P. Baddipadiga, P. Fajri, and M. Ferdowsi, "An overview of direct current distribution system architectures & benefits," *Energies*, vol. 11, p. 2463, 09 2018.

[10] A. Shekhar, L. Mackay, L. Ramirez-Elizondo, and P. Bauer, "State space model for n-parallel connected dc-dc converters with predictive current control strategy," in *PCIM Europe 2016; International Exhibition and Conference for Power Electronics, Intelligent Motion, Renewable Energy and Energy Management*, 2016, pp. 1–8.

[11] Z. Wang and Y. Chen, "Design of a high efficiency buck converter," in *2020 IEEE 1st China International Youth Conference on Electrical Engineering (CIYCEE)*, 2020, pp. 1–6.

[12] J. Roy, A. Gupta, and R. Ayyanar, "Discontinuous conduction mode analysis of high gain extended-duty-ratio boost converter," *IEEE Open Journal of the Industrial Electronics Society*, vol. PP, pp. 1–1, 05 2021.

[13] L. Palma, M. Todorovic, and P. Enjeti, "Design considerations for a fuel cell powered dc-dc converter for portable applications," in *Twenty-First Annual IEEE Applied Power Electronics Conference and Exposition, 2006. APEC '06.*, 2006, pp. 6 pp.–.

[14] K. Górecki and K. Detka, "Analysis of influence of losses in the core of the inductor on parameters of the buck converter," in *2018 Baltic URSI Symposium (URSI)*, 2018, pp. 129–132.

[15] F. A. Fayrouz, M. A. Elgendy, M. Dahidah, and M. Muhammad, "Analysis of dcm interleaved boost converter for pv ac-module application," in *The 10th International Conference on Power Electronics, Machines and Drives (PEMD 2020)*, vol. 2020, 2020, pp. 343–348.

[16] A. Mukkapati and V. Krishnasamy, "Design and analysis of high gain buck-boost converter topology with reduced voltage stress," *2019 National Power Electronics Conference (NPEC)*, 2019.

[17] N. Mohan, T. M. Undeland, and W. P. Robbins, *Power Electronics: Converters, applications, and design*. Wiley, 2003.

[18] "Ihlp inductor loss calculator tool," https://www.vishay.com/en/inductors/calculator/calculator/, accessed: 2023-04-12.

[19] L. Jeremy, C. A. Ooi, and J. Teh, "Non-isolated conventional dc-dc converter comparison for a photovoltaic system: A review," *Journal of Renewable and Sustainable Energy*, vol. 12, p. 013502, 01 2020.

[20] J. P. M. Figueiredo, F. L. Tofoli, and R. L. Alves, "Comparison of nonisolated dc-dc converters from the efficiency point of view," in *XI Brazilian Power Electronics Conference*, 2011, pp. 14–19.

[21] H.-L. Do, "Zero-voltage-switching synchronous buck converter with a coupled inductor," *IEEE Transactions on Industrial Electronics*, vol. 58, no. 8, pp. 3440–3447, 2011.

[22] D. Butnicu and L.-C. Lazăr, "An efficiency comparative workbench study of egan and silicon discrete transistor based buck converters," in *2020 IEEE 26th International Symposium for Design and Technology in Electronic Packaging (SIITME)*, 2020, pp. 350–353.